Ferroelectricity Induced by Oxygen Isotope Exchange in Strontium Titanate Perovskite

M. Itoh,[1,*] R. Wang,[1] Y. Inaguma,[1] T. Yamaguchi,[2] Y-J. Shan,[3] and T. Nakamura[3]
[1]*Materials and Structures Laboratory, Tokyo Institute of Technology, 4259 Nagatsuta, Midori, Yokohama 226-8503, Japan*
[2]*Department of Electrical Engineering, Faculty of Science and Engineering, Meisei University, Hodokubo, Hino, Tokyo 191-8506, Japan*
[3]*Department of Applied Chemistry, Faculty of Engineering, Utsunomiya University, 7-1-2 Yoto, Utsunomiya 321-8585, Japan*
(Received 28 December 1998)

Ferroelectricity was induced in $SrTiO_3$ by the isotope exchange of ^{18}O for ^{16}O. Dielectric measurements confirmed the ferroelectricity of $SrTi^{18}O_3$, showing a peak at 23 K. A hysteresis loop in the D vs E measurement and TO phonon observed in the Raman spectra supported the evolution of ferroelectricity in $SrTi^{18}O_3$. This is the first demonstration of $SrTiO_3$ becoming ferroelectric without the application of external fields or the introduction of a random field through cation substitution. [S0031-9007(99)08960-7]

PACS numbers: 77.80.Bh, 77.84.Dy

Stimulated by the discovery of high-T_c superconductivity in layered perovskite cuprates, extensive studies have been conducted on perovskite and related oxides not only for application to practical devices but also for elucidating and exploring exotic new properties of oxides. Recently, a high level of piezoelectricity was found in $SrTiO_3$ (STO) [1], whose piezoelectric response increases at low temperatures and at 1.6 K is comparable to that of the best materials at room temperature. STO is one of the most widely studied materials in solid state physics and chemistry, as it exhibits interesting properties including (a) quantum paraelectricity [2], (b) induced ferroelectricity by an electric field [3], uniaxial stress [4], Ca substitution [5], and (c) zone boundary phase transition [6]. Quantum paraelectric behavior is well known for $KTaO_3$ [7] and $SrTiO_3$ [8]. The dielectric constant, ε_r, in quantum paraelectric $SrTiO_3$ perpendicular to the c axis, increases to about 30 000 upon cooling, and then remains temperature independent below 3 K because of quantum fluctuations. From the viewpoint of crystal stability, the induced ferroelectricity of STO originates from the critical status of this material. The tolerance factor, $t = (r_{Sr} + r_O)/\sqrt{2}\,(r_{Ti} + r_O)$, where r_i is the ionic radius of ion i, is an effective parameter for evaluating the properties of perovskites. Using the Shannon radii [9] we obtain $t = 1.00$ for STO, which means that the ion packing in STO is ideal for a perovskite-type structure. Larger and smaller values of t in titanate perovskites favor ferroelectricity [cf. $BaTiO_3$ (BTO)] and quantum paraelectricity [cf. $CaTiO_3$ (CTO) [10]], respectively. The critical status of STO is reflected in both the high polar state observed in BTO and quantum paraelectricity observed in CTO. The zone boundary phase transition of STO, which originates from condensation of the R_{25} zone boundary soft mode [11], has been a fascinating theme in the soft mode theory. The zone boundary phase transition of STO at 105 K does not coincide with the anomaly in the dielectric constant that occurs with changes in temperature; the manifestation of the transition was demonstrated by the electron resonance technique [12] and by neutron diffraction analysis [11].

The recent efforts of our group have been devoted to the discovery of ferroelectrics in the perovskites. In the course of classifying known materials for the perovskite titanates, a new parameter, the average mass of the A-site ion, was found to be a determining factor for the evolution of ferroelectricity in these compounds [13]. Based on this scheme, ferroelectricity appears only in regions in which the average atomic masses of the A-site ions are $M_A > 100$, suggesting the importance of mass balance between A and TiO_3; i.e., the Last mode [14] is important in the evolution of the perovskite titanates. Because $M_{TiO_3} = 47.9 + 16.0 \times 3 = 95.9$, the condition $M_A > 100$ suggests the importance of relative amplitude of A and TiO_3. Based on such criteria, we have become aware of the important role that mass plays in the vibrating system, a role that may be a crucial factor for the evolution of ferroelectricity. In addition to the Last mode, the Slater mode [15], which is the relation, vibration of Ti vs O_3, also plays an important role in the evolution of ferroelectricity. Previous studies have suggested that an admixture of these two modes play a role in the evolution of ferroelectricity in $PbTiO_3$ and $BaTiO_3$ [16]. On further reflection, the mass ratio between Ti and O_3 is crucial if our classification for the known ferroelectrics is justifiable. That is, the mass ratio $47.9/48.0 \approx 1$ for Ti/O_3 may play an important role in the evolution of quantum fluctuation. Deviation of the ratio from unity in both A/TiO_3 and Ti/O_3 may increase the nonlinear response of the vibrating system to the external field, contributing to a softening of the modes. We have attempted to modify STO to favor the ferroelectric state by means of oxygen isotope substitution, and, as a result, we have found that substitution of ^{18}O for ^{16}O induces ferroelectricity at temperatures below 23 K.

The experiments were performed on a single-crystal plate of STO, 3 mm by 3 mm by 0.4 mm, cut from a single crystal lump, whose edges were parallel to those

 0031-9007/99/82(17)/3540(4)$15.00

of a [100] cubic. The impurities in the crystal were less than 1 ppm. Polycrystalline STO was also prepared by the conventional solid state reaction technique to check changes in the lattice constant after the isotope exchange. Determination of the lattice constant for the polycrystalline sample was carried out using Si powder (6N) as an internal standard. This crystal was heated in an $^{18}O_2$ gas (Isotech, Co.) with 99% purity for more than one week. The final exchange rate was measured from the weight increase. Two samples were subjected to the isotope exchange, and their exchange ratios were 93% (STO18) and 45% (STO18-45). The sample STO18-45 was sealed in a quartz tube under vacuum and annealed for 10 days at 1273 K to confirm the homogeneity of the oxygen isotopes. Both faces of the crystal were pasted with gold paste and fired at 600 °C in $^{18}O_2$ atmosphere. The capacitance of the crystals, $SrTi^{16}O_3$(STO16), STO18-45, and STO18, were measured using an HP4284A LCR meter with an applied measuring field of 1 V peak-to-peak in a temperature range from 1.6 to 300 K. Measurements of the D vs E loop and the pyroelectricity of the samples were carried out using a handmade circuit and a Keithley 6517 electrometer/high resistance meter, respectively. Raman spectra for STO16 and STO18 were recorded at 4, 10, and 50 K using a Jobin-Yvon microscopic laser Raman spectrometer with an Ar coherent light of $\lambda = 514.53$ nm at 0.05 mw power by means of backscattering. The laser beam size was about 1 μm. To check the phase-transition temperature, a heat capacity measurement was carried out using a Quantum Design PPMS heat capacity measurement module.

The results of the measurements of dielectric constants ε_r are shown in Fig. 1. The dielectric constant peaked at slightly different temperatures between 23.2 K for 10 kHz and 23.5 K for 100 kHz. In the high temperature range, when fitting $100 < T < 200$ K, ε_r vs T showed classical-Curie-Weiss-type behavior, as demonstrated by the linearity of $1/\varepsilon_r$(100 kHz) vs T in Fig. 1. Another fit with a Barrett-type quantum paraelectric law [2], $\varepsilon_r(T) = A/[(T_1/2)\coth(T_1/2T)\text{-}T_0]$ for STO18, gave the fitting parameters $A = 1.2886 \times 10^5$, $T_1 = 87$ K, and $T_0 = 44$ K. These parameters are similar to those found for pure $SrTiO_3$, $T_1 = 84$ K and $T_0 = 38$ K [17], with the subtle difference that the ^{18}O substitution makes $T_1 - 2T_0$ negative, an indicator of ferroelectricity. The ε_r peak for STO18 appeared at around 23 K, as shown in Fig. 1, which is almost the same as the peak temperature of the Ca-substituted system, 18 K [5]. The peak in ε_r and the large $\tan\delta$ for STO18 suggest that this crystal is a ferroelectric, below 23 K. ε_r for STO18-45 showed very broad peaks below 10 K. Bednorz *et al.* have reported the appearance of T_c for the Ca-substituted compound $Sr_{0.993}Ca_{0.007}TiO_3$ at 18 K both by dielectric measurement [18] and by Raman spectroscopy [19]. When we compare the dielectric behaviors of Ca-substituted STO (CSTO) with STO18, we recognize the following differences:

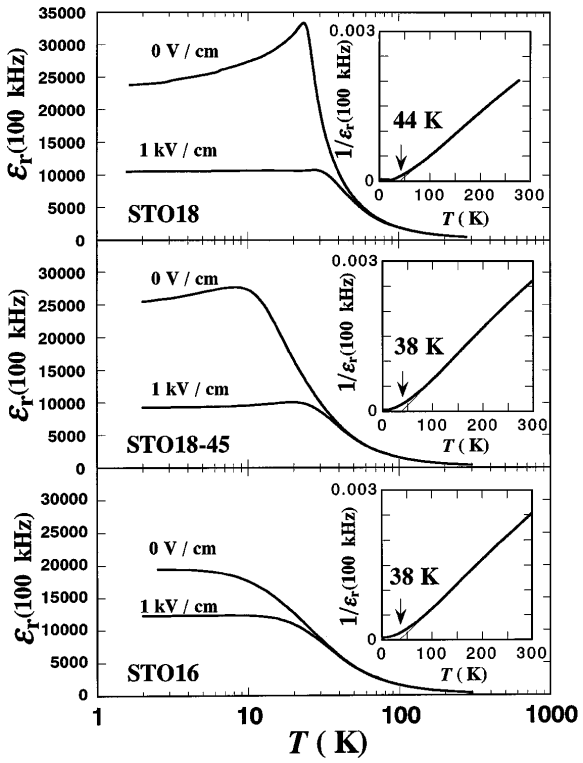

FIG. 1. Comparison of temperature dependence of ε_r and $\tan\delta$ for STO16, STO45-18, and STO18. Insets show the temperature dependence of $1/\varepsilon_r$ for zero bias. Temperatures in the insets show θ obtained by the least squares fitting by Curie-Weiss law, $\varepsilon_r = C/(T - \theta)$, for the data between 100 and 200 K.

(1) ε_r for CSTO is fairly large, $\varepsilon_r \approx 110\,000$, whereas it is 33 000 to STO18. (2) The asymptotic Curie temperatures differ from each other, 18 K for CSTO (20–30 K) and 44 K for STO18 (100–200 K), which is higher than the 38 K for STO16 and STO18-45.

Another important result obtained in this study is the change in ε_r with bias voltage. This effect has been pointed out for STO [20] and CSTO [18]. With increasing bias voltage, ε_r for STO16 decreases but is still constant below a certain temperature. A higher bias voltage, which is high enough to distort the crystal into lower symmetry, is expected to change STO16 to a ferroelectriclike state [20]. The ferroelectriclike ε_r peak for STO18 disappears as the bias voltage increases. ε_r changes to show a quantum paraelectriclike behavior under bias voltage. Application of the bias in the same direction as the ε_r measurement may harden the oscillation system. In such a case the quantum paraelectric phase becomes more favorable from an energetic point of view since the vibrational energy level interval expands.

To confirm the ferroelectricity of STO18, the D vs E loop and the pyroelectricity were measured, and the former result is shown in Fig. 2. It is clearly shown that the hysteresis loop disappears above 45 K and only a nonlinear curve remains. It is well known that a D vs E hysteresis loop can also be observed for STO16

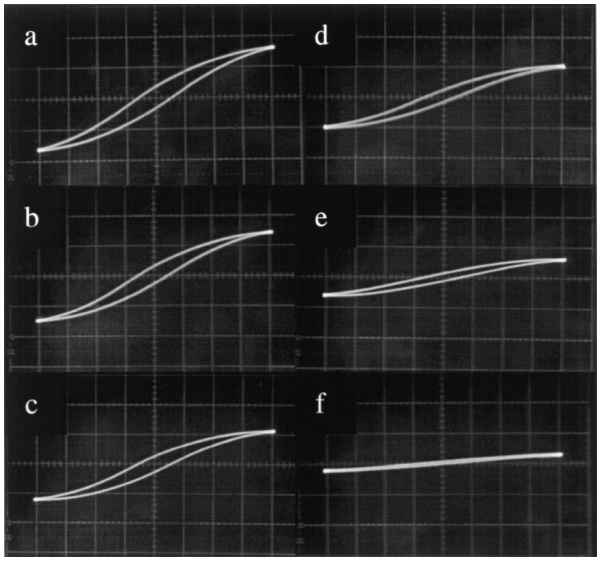

FIG. 2. D vs E loops for STO18 measured at 18.1 K (a), 20.2 K (b), 24.2 K (c), 28.6 K (d), 35 K (e), and 45.5 K (f). 1 division = 1.04 kV/cm and 0.901 μC/cm^2, for E and D, respectively.

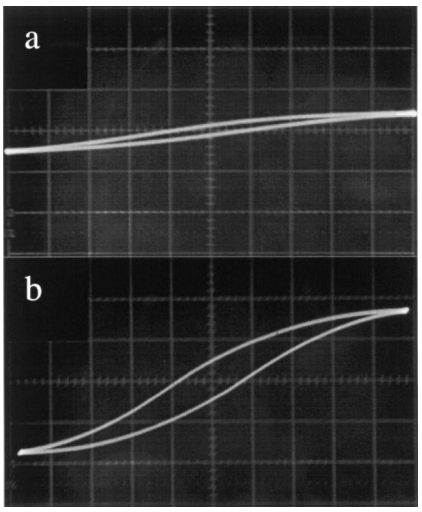

FIG. 3. Comparison of D vs E loops for STO16 (a) and STO18 (b) measured at almost the same conditions. 1 division = 1.11 kV/cm and 0.849 μC/cm^2 for E and D, respectively, in (a), and 1 division = 1.11 kV/cm and 0.849 μC/cm^2 for E and D, respectively, in (b).

that originates from the induced ferroelectricity caused by the applied high electric field [3]. Figure 3 shows a comparison of the D vs E loops for STO16 and STO18 at 18 K. P_s for STO16 measured at the same conditions as STO18 was about one-third that of STO18. Measurement of the pyroelectricity gave the same result.

At 105 K, a cubic-tetragonal transition occurs in STO16 from cubic (O_h^1) to tetragonal phase with an inversion center (D_{4h}^1) that is not ferroelectric. Application of uniaxial stress or an electric field to the tetragonal phase lowers the symmetry to orthorhombic (C_{2v}) [4]. This decrease in symmetry has also been confirmed in the ferroelectric Ca-substituted system by Raman scattering [19]. Figure 4 shows the Raman spectra of STO18 measured at 4, 10, and 50 K. Because of the crystal subdivisions into domains with a and b axes in the ferroelectric phase, different scattering geometries are probed simultaneously and there are no sharp selection rules. Two intense modes below 20 cm^{-1} can probably be attributed to the TO_1 phonon. These modes are softened with decreasing temperature. At 50 K, these two modes disappear. A more precise determination of the temperature dependence of the Raman scattering may be required, but at the present time we could not check the temperature difference between the thermometer of the cryostat and the temperature of the sample where the Ar laser beam was irradiated.

In Fig. 5, we have comparatively shown the heat capacities for STO16, STO18-45, and STO18. Except for STO18, no heat anomaly due to phase transition was observed below 100 K. In order to clarify our results, differences in the heat capacities of STO16 and STO18 are shown in Fig. 5(a), and C_p/T is shown in Fig. 5(b). Two important points are made clear in this figure: (1) The heat anomaly at 42 K is observed only with STO18. (2) The cubic-tetragonal phase transition temperature is increased from 105 K for STO16 to 110 K for STO18. (3) The diffuse transition in STO18-45 and STO18 comes from the randomness of ^{16}O and ^{18}O in the oxygen site. The heat anomaly at 42 K may correspond to a phase transition, leading to the lowering of the crystal symmetry from tetragonal to a lower one. The very small heat anomaly may correspond to the displacive character of the phase transition, which is caused by the shift of constituent ions. It was found that the heat anomaly at 42 K became diffuse after several rounds of thermal cycling, but it was always observed for virgin crystal which did not experience the

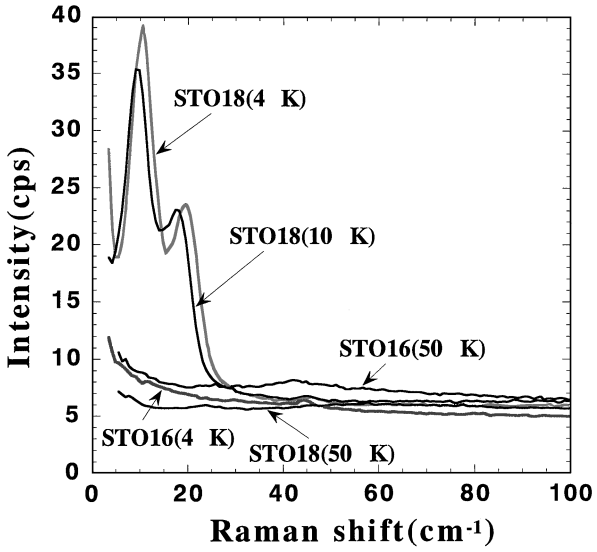

FIG. 4. Raman spectra for STO16 and STO18 at 4, 10, and 50 K.

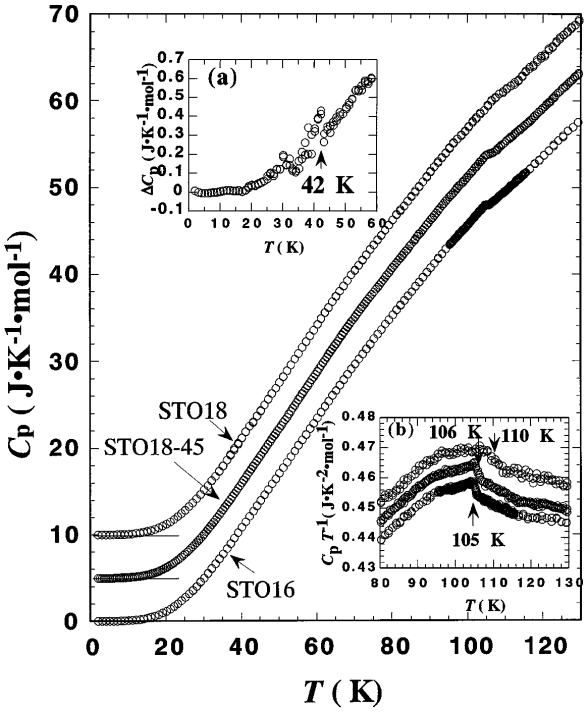

FIG. 5. Heat capacities for STO16, STO18-45, and STO18. Insets (a) and (b) show the difference in C_p values between STO16 and STO18 and C_p/T in the vicinity of 100 K, respectively.

thermal cycling from room temperature down to 2 K. The disappearance of heat anomaly after heat cycling may be related to the formation of crystallographic twins and the breaking of crystallographic domains into small pieces. The lattice parameters for STO16 and STO18 were found to be 3.9054(3) and 3.9052(1) A, respectively. This difference in the lattice parameters is within the range of experimental error. A low temperature structure analysis by powder x-ray diffraction for STO18 showed the structural change at 110 K, but no other change due to phase transition was detected.

Isotope exchange for STO16 has identified the critical state of STO16, which is characterized by quantum paraelectricity instead of ferroelectricity at low temperatures. We have also substituted ^{18}O for ^{16}O in $BaTiO_3$ and $CaTiO_3$ polycrystalline samples. The former showed a 0.9 K increase in T_c and the latter no effect. This result shows that the mass effect is enhanced only in the critical system, STO. Hidaka *et al.* [21] have exchanged Ba and Ti isotopes in $BaTiO_3$ and found a change in T_c as large as 20 K. Compared to these results, the effect of oxygen isotope exchange is small and may suggest a prevalence of the Last mode in the contribution to the ferroelectricity in BTO.

Last but not least, additional data on the measurement of ε_r peaks for other samples with different ^{18}O compositions revealed that the peak temperature of ε_r linearly increases from (0) K for 40% ^{18}O up to 23 K for 93% ^{18}O with an increase in ^{18}O [22]. This means that the evolution of ferroelectricity in STO18 is due to fairly cooperative mechanism not by impurity effect.

In conclusion, we have shown that ^{18}O exchange for STO induces ferroelectricity below 23 K. To our knowledge, this is the first example of the evolution of ferroelectricity in STO without applying external fields or introducing random field [5] through the cation substitution of *A* site. The importance of the Slater mode was reconfirmed in this study. The phase transition observed at 42 K in C_p measurement is considered to be closely related to the evolution of ferroelectricity at 23 K. A structural analysis using neutron diffraction techniques for a single domain sample may elucidate the mechanism of the evolution of ferroelectricity.

Part of this work was financially supported by JSPS Research for the Future Program in the Area of Atomic-Scale Surface and Interface Dynamics and a Grant-in-Aid for Scientific Research from the Ministry of Education, Science, and Culture.

*Author to whom correspondence should be addressed. Electronic address: m.itoh@rlem.titech.ac.jp

[1] D. E. Grupp and A. M. Goldman, Science **276**, 392 (1997).
[2] J. H. Barrett, Phys. Rev. **86**, 118 (1952).
[3] P. A. Fleury, J. F. Scott, and J. M. Worlock, Phys. Rev. Lett. **21**, 16 (1968).
[4] H. Uwe and T. Sakudo, Phys. Rev. B **13**, 271 (1976).
[5] J. G. Bednorz and K. A. Müller, Phys. Rev. Lett. **52**, 2289 (1984).
[6] F. W. Lytle, J. Appl. Phys. **35**, 2212 (1964).
[7] U. T. Höchli, H. E. Weibel, and L. A. Boatner, Phys. Rev. Lett. **39**, 1158 (1977).
[8] K. A. Müller and H. Burkard, Phys. Rev. B **19**, 3593 (1979).
[9] R. D. Shannon, Acta Crystallogr. Sect. A **32**, 751 (1976).
[10] I-S. Kim, M. Itoh, and T. Nakamura, J. Solid State Chem. **101**, 77 (1992).
[11] R. A. Cowley, Phys. Rev. **134**, A981 (1964).
[12] L. Rimai and G. A. DeMars, Phys. Rev. **127**, 702 (1962).
[13] T. Nakamura, Y-S. Shan, P-H. Sun, Y. Inaguma, and M. Itoh, Ferroelectrics (to be published).
[14] J. T. Last, Phys. Rev. **105**, 1740 (1957).
[15] J. C. Slater, Phys. Rev. **78**, 748 (1950).
[16] G. Shirane, F. Jona, and R. Pepinsky, Proc. IRE **43**, 38 (1955).
[17] E. Sawaguchi, A. Kikuchi, and K. Kodera, J. Phys. Soc. Jpn. **17**, 1666 (1962).
[18] U. Bianchi, J. Dec, W. Keemann, and J. G. Bednorz, Phys. Rev. B **51**, 8737 (1995).
[19] U. Bianchi, W. Kleemann, and J. G. Bednorz, J. Phys. Condens. Matter **6**, 1229 (1994).
[20] E. Hegenbarth, Phys. Status Solidi **6**, 333 (1964).
[21] T. Hidaka and K. Oka, Phys. Rev. B **35**, 8502 (1987).
[22] M. Itoh *et al.* (unpublished).